Chinese Chemical Letters 34 (2023) 107880

Contents lists available at ScienceDirect

Chinese Chemical Letters

journal homepage: www.elsevier.com/locate/cclet

Triphenylamine-based highly active two-photon absorbing chromophores with push-pull systems

Yanqi Ban[a], Linhong Hao[b], Zhenbo Peng[a], Lishui Sun[a], Lihua Teng[b,*], Yingjie Zhao[a,*]

[a] College of Polymer Science and Engineering, Qingdao University of Science and Technology, Qingdao 266042, China
[b] College of Mathematics and Physics, Qingdao University of Science and Technology, Qingdao 266061, China

ARTICLE INFO

Article history:
Received 5 July 2022
Revised 31 August 2022
Accepted 4 October 2022
Available online 9 October 2022

Keywords:
Star-type chromophores
Triphenylamine derivatives
Two-photon absorption
Nonlinear optical materials
Push-pull systems

ABSTRACT

Two triphenylamine-based star-type push-pull chromophores (**T1**, **T2**) were designed and synthesized. Triphenylamine serves as the central core and acts as an electron-donating group surrounded by electron-withdrawing pentafluorobenzene or *N*,*N*-dimethyl substituted tetrafluorobenzene, which are connected by ethylene bridges. Single-crystal X-ray diffraction confirmed the structures and molecular arrangement of two chromophores. The systematic photophysical research of **T1** and **T2** absorption characteristics was carried out to gain a better understanding of how structure-property relationships affect the observed nonlinear optical absorption phenomenon. Complementary calculations based on density functional theory (DFT) further confirmed the experimental results. Both chromophores exhibited excellent two-photon absorption (TPA) properties in CH_2Cl_2. Notably, **T2** has more remarkable nonlinear optical absorption effects with the TPA cross-section up to 4.24×10^7 GM. By adjusting the electronic structures of the chromophores through introducing pentafluorobenzene or *N*,*N*-dimethyl as functional groups with different electron-donating or withdrawing behaviors, the TPA performance of the small organic molecule could be greatly enhanced. These molecular structures with push-pull systems were excellent candidates for different two-photon applications.

Two-photon absorption (TPA) is a nonlinear optical (NLO) phenomenon in which two photons are simultaneously absorbed by a molecule, causing excitation under intense laser pulses [1]. Organic molecules with large two-photon absorption cross-sections have occupied a significant position among the numerous classes of nonlinear optical materials due to their abundant substituents, high symmetry and multidimensionality [2–6]. The organic TPA molecules have shown various applications in photonics, optoelectronics, photodynamic therapy and bio-imaging, *etc*. [7–11].

Chromophores with strong and universal TPA characteristics are highly desirable for these applications. Numerous studies have shown that triphenylamine derivatives are becoming promising TPA materials [12,13]. Triphenylamine is a well-known strong electron-rich donator with C3 symmetry and outstanding hole-transporting properties that make it a popular TPA scaffold [14–18]. It has been reported that the central nitrogen introduced electron-withdrawing substituents at three pare-positions would be beneficial to obtaining efficient TPA fluorophores [19,39]. Zhou's group synthesized six multi-branched triphenylamine derivatives with the different numbers of the electron-donating group isophorone's branch and applied them in the study of linear and nonlinear optical properties [20]. They noted that TPA cross-sections increased with the electron-donating group's branch number. The compound with C3 symmetry and the largest number of branches has the highest TPA cross-section. Suzuki *et al*. reported the comprehensive investigation of the influence of monosubstituted on two-photon absorption for diphenylacetylene derivatives [21]. Hu synthesized two conjugated organic molecules with excellent TPA properties and emphasized the equal importance of the high TPA cross-section, fluorescent emission and heat dissipation for designing functional TPA molecules [22].

For plenty of small organic molecules, the molecular nonlinearities originate from delocalized electrons in their π-conjugated systems. More abundant and structurally diverse molecules are added with electron-donor (D) and electron-acceptor (A) groups to the ends or centers of the π-conjugated backbone, which can favor electron delocalization and help the excitation of molecules from the ground state to an excited state [23–27]. These simple and effective designs enable chromophores to have large TPA cross-sections to expand the development of NLO materials [28–32]. The electron transfer or electron separation in these D-A-containing

* Corresponding authors.
E-mail addresses: tenglihua80@163.com (L. Teng), yz@qust.edu.cn (Y. Zhao).

https://doi.org/10.1016/j.cclet.2022.107880
1001-8417/

systems of triphenylamine-based derivatives endowed this class of chromophores with highly anisotropic and interesting photophysical properties. Numerous triphenylamine derivatives with dipolar chromophores were synthesized to explore the structure and TPA property relationships by introducing various donor-π-acceptor systems, different π-bridging centers and donor-acceptor strengths [33–35]. It is well known from the literature that electron-withdrawing groups of triphenylamine derivatives mainly focused on cyano, benzothiazole, nitro, and so on could enhance two-photon absorption [36–38]. These organic chromophores, especially with asymmetrical structures and large dipole moments may lead to reduced optical nonlinearity [20]. Consequently, improving molecular symmetry and weakening molecular dipole-dipole interactions were important for enhancing the nonlinear optical properties of chromophores. Aromatic hydrocarbons could be effectively reduced the electron cloud density and weakened polarizability by introducing the most non-metallic fluorine atom. Fluorinated aromatic rings were valuable groups with strong electron-withdrawing effects and large steric hindrances, which could prepare chromophores with push-pull systems. Additionally, fluorinated aromatic rings could play an important role in the nonlinear optical chromophores due to their high thermal stability, low dielectric constants, and good optical transparency [40,41]. However, studies on fluorinated aromatic rings as the electron-withdrawing groups are rarely reported.

Herein, we designed and synthesized two triphenylamine-based TPA molecules: star-shaped ((A-π-)3D) (**T1**) [42] and star-shaped ((D-A-π-)3D) (**T2**) molecules (Fig. 1a). The single-crystal structures of **T1** and **T2** grown from different solvents were obtained. Triphenylamine was chosen as the core to construct branched molecules and indicated prominent electron-donating ability. Pentafluorobenzene (ArF) unit as an electron acceptor was then introduced at three pare-positions to the central nitrogen forming (A-π-)3D model structure. The electron transfer between the triphenylamine and ArF contributes to the interesting linear or nonlinear photophysical properties of **T1**. This also implies that the star-shaped ((A-π-)3D) structures could offer substantial delocalization of π-electrons and controllable charge separation.

Based on the chromophore of **T1**, extending the π-electron conjugated system and improving the solubility by introducing *N*,*N*-dimethyl to the pentafluorobenzene lead to **T2** [43]. **T2** was chosen to investigate the effects of the π-conjugated spacer length on the optical properties. The *N*,*N*-dimethyl as an electron-donating group will make the whole structure more balanced in charge recombination and change the polarizability of electrons in frontier molecular orbitals. **T1** and **T2** show typical intramolecular charge transfer (ICT) effects. Whereas, the optical properties (especially two-photon absorption and two-photon excited fluorescence) of these compounds have not been investigated in-depth, let alone the influence of structures on photophysical properties. Therefore, we systematically analyzed their linear and nonlinear optical properties and further explored the relationship between structure and optical properties. When compared with other reports, this work showed that both **T1** and **T2** demonstrated excellent TPA phenomenon in CH_2Cl_2, especially at low power (Table S1 in Supporting information). Moreover, **T2** exhibits more remarkable nonlinear optical absorption effects with the TPA cross-section up to 4.24×10^7 GM. Theoretical DFT computational indicates that the bulky ArF group and long conjugation length contribute to improved TPA and emission activity really. The synthesis of **T1** and **T2** is very straightforward. **T1** and **T2** were synthesized by a two-step reaction to give the final products (Scheme S1 in Supporting information). For the synthesis details, see the supporting information. Both **T1** and **T2** show good solubility in common organic solvents.

T1 and **T2** could be easily crystallized from different solvents. The single crystals of molecules **T1** and **T2** suitable for X-ray diffraction analysis were successfully obtained. **T1** was grown by the slow evaporation of *n*-hexane into CH_2Cl_2 solution at room temperature. While the single crystal of **T2** was acquired through evaporation of tetrahydrofuran solution, CH_2Cl_2 solution or cooling down the toluene solution slowly. As shown in Figs. 1b and c, the single-crystal X-ray diffraction confirms the molecular structures and spatial arrangements of **T1** and **T2** (**T1**, **T2**, **T2**_CH_2Cl_2, **T2**_toluene). The single-crystal structures of **T1** and **T2** with or without solvent molecules. For the structure of **T1**, the crystal structure belongs to the *P*1 space group with unit cell parameters of $a = 11.61$ Å, $b = 12.12$ Å, $c = 12.94$ Å, $\alpha = 94.80^\circ$, $\beta = 99.38^\circ$, $\gamma = 109.11^\circ$. A clear 2D layered structure was observed. In each layer, the **T1** molecules were arranged in a head-to-tail formation to form a 1D thread first. The 1D threads were then arranged in a head-to-head formation alternately to form a 2D layer. The **T2** crystal belonged to space group *P*1 and the unit cell parameters

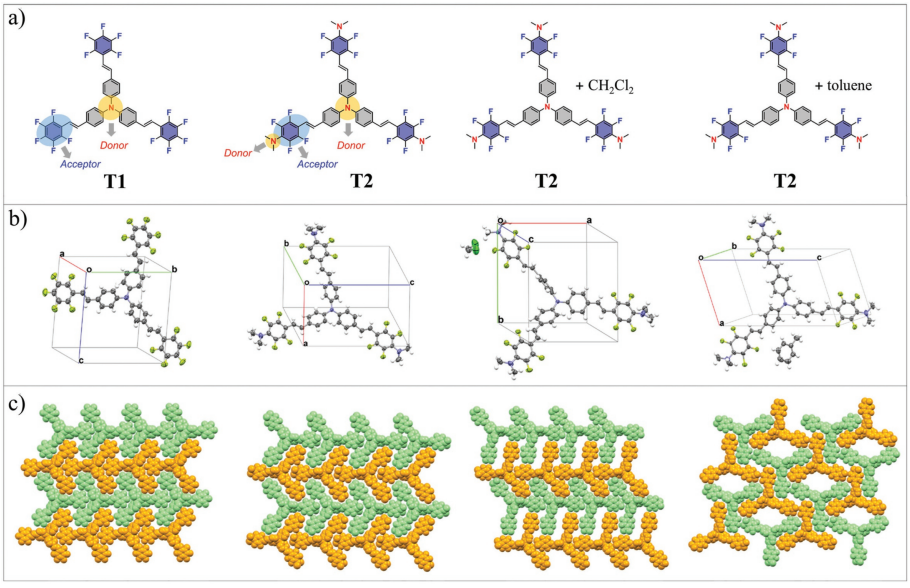

Fig. 1. (a) Chemical structures of molecules **T1** and **T2**. (b) The corresponding single-crystal structures of **T1** and **T2** from different solutions. (c) The crystal-packing arrangement of **T1** and **T2**.

are $a = 9.67$ Å, $b = 13.71$ Å, $c = 16.33$ Å, $\alpha = 103.38^{\circ}$, $\beta = 90.88^{\circ}$, $\gamma = 104.04^{\circ}$. Crystal **T2** has the almost same self-assembly mode as **T1**, although **T2** was obtained from tetrahydrofuran (THF). For the crystal of **T2**_CH_2Cl_2, a slightly different packing mode was adopted, and some subtle slippage between some 1D threads was observed. The 2D layered structure was still achieved in the end. The crystal of **T2**_CH_2Cl_2 belonged to space group $P1$, with unit cell parameters $a = 11.94$ Å, $b = 13.47$ Å, $c = 14.14$ Å, $\alpha = 88.21^{\circ}$, $\beta = 72.92^{\circ}$, $\gamma = 89.83^{\circ}$. However, for the crystal of **T2**_toluene with a solvent molecule of toluene, a completely different packing mode was adopted. More interspace in each 2D layer was observed. The crystal of **T2**_toluene also belonged to space group $P1$, with unit cell parameters $a = 10.79$ Å, $b = 13.58$ Å, $c = 17.73$ Å, $\alpha = 68.57^{\circ}$, $\beta = 72.97^{\circ}$, $\gamma = 74.49^{\circ}$. The supporting information provides detailed information about the single-crystal X-ray diffraction data.

All the crystals belonged to space group $P1$ with a propeller-shaped structure, which is a typical feature of triphenylamine derivatives. The dihedral angles between the benzene rings of central triphenylamine and peripheral phenyl ring with *N*,*N*-dimethyl is 21.37° in **T2**_CH_2Cl_2, whereas the dihedral angles located in the same positions are 38.23° in **T2**, 29.38° in **T2**_toluene (Fig. S1 in Supporting information). The dihedral angles between the benzene rings of central triphenylamine and pentafluorobenzene rings are 31.08° in **T1** (Fig. S1). These results showed that the crystal of **T2**_CH_2Cl_2 possessed better planarity than other crystals. Therefore, the electron mobility in the conjugate system was increased as well as the TPA cross-section. The better planarity of **T2**_CH_2Cl_2 is beneficial to light absorption properties, which was consistent with the experimental results.

The photophysical properties of **T1** and **T2** were studied. The UV-vis absorption spectra of the **T1** and **T2** exhibit two distinct maximum absorption peaks at 283 and 400 nm for **T1**, 319 and 405 nm for **T2** in CH_2Cl_2 solution (Fig. 2a). The lower wavelengths in the high-energy region are assigned to the absorption of the π-π^* transitions caused by the triphenylamine core. The higher wavelength peaks are ascribed to the absorption of the intramolecular charge transfer (ICT). **T2** shows a slight red-shift at the maximum absorption peaks. This is a characteristic behavior of ICT bands induced by the electron-donating group of *N*,*N*-dimethyl. Besides, two chromophores have nearly independent on the nature of the solvent (Fig. S2 in Supporting information). According to the UV-vis spectra, the bandgap of **T1** and **T2** were calculated to be 2.79 eV and 2.76 eV, respectively (Fig. S3 in Supporting information). The fluorescence emission spectra of **T1** and **T2** displayed the maximum emission of 499 and 504 nm (Fig. 2b). The fluorescence intensity of **T2** was slightly higher than **T1**. The emission spectra of **T1** and **T2** in CH_2Cl_2 followed a similar trend to that observed for the absorption spectra. As shown in Fig. S4 (Supporting information), the solid-state UV-vis spectra revealed that four crystals showed a broad absorption range from 350 nm to 450 nm. Solid-state fluorescence spectra of crystals of **T1** and **T2** displayed the maximum emission of 489 and 515 nm.

Two-photon excited fluorescence experiments were performed by using 60-fs pulses from a Ti: sapphire laser operating at 800 nm with the repetition rate of 80 MHz. The strong green-fluorescent photon emissions of two molecules can be observed, as shown in Fig. 2c. **T1** and **T2** exhibit maximum fluorescent emission features at 493 and 497 nm, respectively, which means both molecules emit photons with significantly higher energy than that of their excitation photon. Since the UV-visible absorption of the two compounds displays almost no absorption above 460 nm, this indicates that the fluorescence emission creased by femtosecond laser pulse arises from a nonlinear optical two-photon absorption process. Additionally, at the same excitation intensities, the fluorescence intensity of **T2** was stronger than **T1**. The stronger emission ability of **T2** meant a better TPA efficiency than **T1**. The crystals of **T1** and **T2** exhibited maximum fluorescent emission features at 501 and 503 nm under the excitation of an 800 nm femtosecond laser, which indicated that all crystals had a nonlinear optical absorption phenomenon (Fig. S4). However, due to the rough surfaces of prepared solid fibrous samples, many lasers were lost seriously in the OA Z-scan experiment. The nonlinear optical parameters of the crystals could not be measured accurately. The electrochemical studies have been performed, however, the cyclic voltammetry (CV) curves indicated the irreversible electrode process of two chromophores. **T2** (0.86 V) had a lower onset oxidation potential than **T1** (0.97 V), due to the introduced electron-donating groups *N*,*N*-dimethyl (Fig. S5 in Supporting information).

To obtain the frontier molecular orbital information of chromophores **T1** and **T2**. In this study, density functional theory (DFT) calculations were carried out on two compounds using Gaussian 03 software with B3LYP/6-311G (d, p) basis sets [44]. The geometries, as well as the HOMO/LUMO and ground-state dipole moments, are shown in Fig. S6 (Supporting information). The higher HOMO level of **T2** is in good agreement with the electrochemical results and confirms that **T2** presents a lower onset oxidation potential. The HOMO and LUMO diagrams clearly show a typical ICT process in the two compounds. In the triphenylamine core, the electron clouds of the HOMO are evenly distributed. Although the electron clouds of the HOMO are evenly distributed in the triphenylamine core, the majority of electron clouds of the LUMO are transferred and evenly distributed in the branched. The energy gaps ΔE calculated by DFT for chromophores **T1**-**T2** were 3.012 eV and 2.965 eV, respectively. The ΔE indicated that chromophores **T2** has a bigger maximum absorption wavelength in UV-vis spectra, which is consistent with the results of experimental UV-vis spectra analysis.

The nonlinear optical properties of the **T1** and **T2** were measured by the open aperture (OA) Z-scan technique. The schematic of the experimental setup was shown in Fig. S7 (Supporting information). In this open aperture Z-scan experiment, the light source was the 800 nm Ti: Sapphire femtosecond laser, samples were held in a quartz cuvette with 1 mm path length and the pulses are focused into the sample cell with a 200 mm focal length lens. Upon moving the sample cell along the beam across the focal point, the

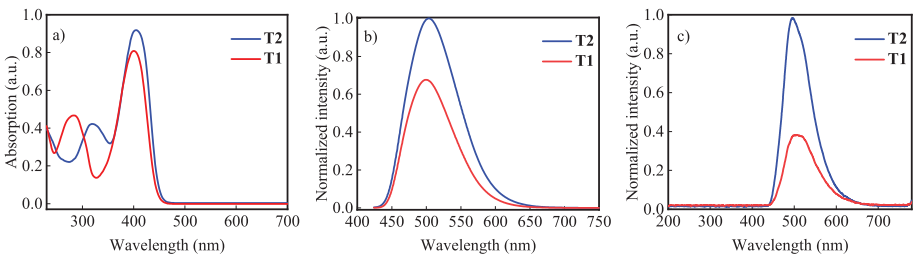

Fig. 2. (a) UV-vis absorption spectra and (b) fluorescence spectra of **T1** and **T2** in CH_2Cl_2 (1.0×10^{-5} mol/L). (c) TPA emission spectra of **T1** and **T2** under the excitation of an 800 nm femtosecond laser and their comparison.

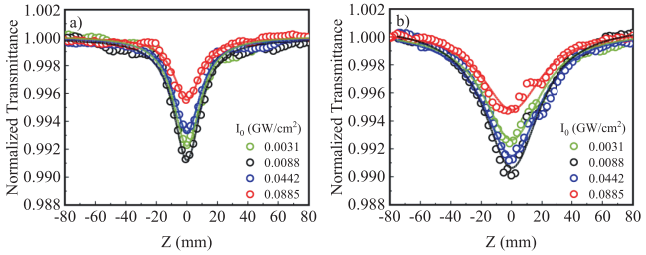

Fig. 3. OA Z-scan results for (a) **T1** and (b) **T2** at different excitation intensities at the focal point $I_0 = 0.0031$ GW/cm^2, 0.0088 GW/cm^2, 0.0442 GW/cm^2, 0.0885 GW/cm^2. The circles are experimental results. The solid lines show the theoretical fitting.

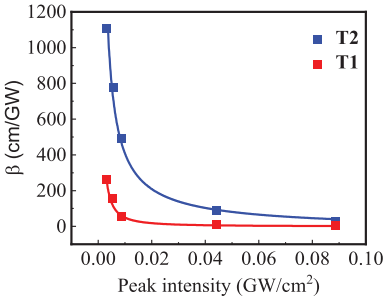

Fig. 4. Measured effective TPA coefficient β of **T1** and **T2** as functions of intensity.

transmittance beam was detected by using a silicon photodetector. More details of other OA Z-scan experimental datasets are provided in Table S2 (Supporting information).

Under these conditions, the observed large NLA of two chromophores mainly resulted from the molecules themselves because the CH_2Cl_2 did not express any nonlinearity used for the nonlinear absorption measurement. It is well known that as the sample approaches the focal point, nonlinear effects will appear due to high intensity/fluence [45]. Different nonlinear mechanisms can lead to the decrease of sample transmittance (reverse saturation absorption (RSA)) or to the increase of sample transmittance (saturable absorption (SA)) [46,47]. The transition energies (between S_0 and S_1) of the two chromophores (**T1**, **T2**) were calculated to be 3.011 and 2.935 eV, respectively. When excited at 800 nm (1.55 eV), electrons in the ground state simultaneously absorbing two photons can be excited to the excited state. In addition, since the wavelength of 800 nm locates outside the absorption band of two chromophores, one-photon-induced excited-state absorption can be negligible. Hence, TPA is the main mechanism for two chromophores at 800 nm. The normalized transmission profiles of **T1** and **T2** with a concentration of 1.0×10^{-5} mol/L in CH_2Cl_2 (Fig. 3). The experimental curves of the two chromophores under different excitation intensities show interesting regularities. The curves exhibit an RSA process induced by TPA with a valley located at zero position (focal point). The TPA will be enhanced with the increasing excitation intensity while the transmittance should decrease. However, as the excitation intensity increased from 0.0088 GW/cm^2 to 0.0885 GW/cm^2, the transmittance increased from 0.991 to 0.996. The abnormal phenomenon may be originated from the saturation of TPA. Electrons are excited to the excited state during the TPA process. The higher the excitation intensity means the higher the electron density. An additional SA component decreases the TPA and increases the transmittance. A similar regularity has also been observed for **T2**. The TPA process becomes saturated at high excitation intensity. The saturation of TPA implies that electrons with high density can be excited to the excited state. Thus, both chromophores possess excellent TPA properties. In addition, the nonlinear absorptive valley of **T2** is extra broadened compared with **T1** signifying an improvement in the nonlinear optical properties.

The TPA coefficients (β) of two molecules can be calculated from the numerical fitting of normalized OA Z-scan transmission, which is described in Eq. 1 [48]:

$$T(Z) = \sum_{n=0}^{\infty} \frac{(-q_0)^n}{(n+1)^{3/2}\left(1+Z^2/Z_0^2\right)^n} \quad (1)$$

where the free factor $q_0 = \beta L_{eff} I_0$, *and* $L_{eff} = \frac{1-e^{-\alpha l}}{\alpha}$, Z_0 is the diffraction length of the beam, L_{eff} is the effective length of the sample and I_0 is the maximum on-axis intensity in the focus ($z = 0$). α_0 denotes the linear absorption coefficient and l represents the thickness of the sample. As shown in Fig. 3, the measured curves can be well fitted by Eq. 1, so that the TPA coefficients can be extracted. The β values of two chromophores shown reduced gradually with excitation intensities increasing (Fig. 4). These results infer that both chromophores possess excellent TPA properties. Since electrons with high density can be excited to the excited state, which can in turn reduce the TPA ability due to the saturation of TPA and the saturation effect of TPA strengthened with the increasing excitation intensity. In addition, β values of **T2** are bigger than **T1** at the same conditions. **T2** has a more remarkable TPA ability. TPA performance could be greatly enhanced by adjusting the pentafluorobenzene electron-donating or *N*,*N*-dimethyl withdrawing groups.

Furthermore, the TPA cross-section (σ) could be determined through the Z-scan measurements by Eq. 2 [49]:

$$\sigma = h\nu\beta \times 10^3 / N_A d \quad (2)$$

where h is Planck's constant, ν is the frequency of input intensity, N_A is the number density of molecules in units of cm^{-3} (0.01 mmol/L in the current case), and d is the molar concentration of the solution. The results of the nonlinear absorption parameters measured are summarized in Table S1. It has been shown that extended π-conjugation could lead to greater densities of populations for both electronic and vibrational states, providing more effective coupling channels, which would in turn increase the TPA cross-section. The TPA cross-section values of **T2** are bigger than **T1** under the same conditions, which implies that it is possible to increase the two-photon absorption properties of **T2** by extending the π-conjugation by simply including *N*,*N*-dimethyl. Both chromophores possessed excellent two-photon absorption σ values at very low input intensity, while **T2** has the largest σ values up to 4.24×10^7 GM at excitation intensity of 0.0031 GW/cm^2. By modulating the structures of the conjugated organic molecules as chromophores, excellent nonlinear properties could be obtained.

In summary, we have systematically studied the nonlinear optical properties of two novel star-type of triphenylamine derivatives. Two chromophores exhibited superior two-photon absorption properties with large TPA cross-sections up to 4.24×10^7 GM at 800 nm, suggesting that molecular structures offer a wide range of possibilities for two-photon applications. The DFT calculations help significantly in the fundamental understanding of the ICT characteristics of **T1** and **T2**. Accordingly, molecules based on the molecular platform of triphenylamine might be able to have even larger TPA cross-sections. This study makes it easier to create novel two-photon absorption-based nonlinear optical devices in the future.

Declaration of competing interest

The authors declare that they have no known competing financial interests or personal relationships that could have appeared to influence the work reported in this paper.

Acknowledgments

This work was supported by the National Natural Science Foundation of China (Nos. 51972185, 12174211, 11874232 and 31202117), the Natural Science Foundation of Shandong Province (No. ZR2020ZD38).

Supplementary materials

Supplementary material associated with this article can be found, in the online version, at doi:10.1016/j.cclet.2022.107880.

References

[1] M. Pawlicki, H.A. Collins, R.G. Denning, H.L. Anderson, Angew. Chem. Int. Ed. 48 (2009) 3244–3266.
[2] L. Liu, Z.Q. Zhou, J.P. Shi, et al., Chin. Chem. Lett. 22 (2011) 1147–1150.
[3] L. Porre's, O. Mongin, C. Katan, et al., Org. Lett. 6 (2004) 47–50.
[4] P. Wei, X.D. Bi, Z. Wu, Z. Xu, Org. Lett. 7 (2005) 3199–3202.
[5] O. Mongin, L. Porre's, C. Katan, et al., Tetrahedron Lett. 44 (2003) 8121–8125.
[6] B.P. Biswal, S. Valligatla, M. Wang, et al., Angew. Chem. Int. Ed. 58 (2019) 6896–6900.
[7] M. Hansel, C. Barta, C. Rietze, et al., J. Phys. Chem. C 122 (2018) 25555–25564.
[8] U.R. Felscia, B.J.M. Rajkumar, P. Sankar, R. Philip, M.B. Mary, Mater. Chem. Phys. 243 (2020) 122466.
[9] W. Zhuang, L. Yang, Ma B, et al., ACS Appl. Mater. Interfaces 11 (2019) 20715–20724.
[10] K.A. Kasischke, H.D. Vishwasrao, P.J. Fisher, W.R. Zipfel, W.W. Webb, Science 305 (2004) 99–103.
[11] X. Li, Z. Li, Y.W. Yang, Adv. Mater. 30 (2018) 1800177.
[12] C. Katan, F. Terenziani, O. Mongin, J. Phys. Chem. 109 (2005) 3024–3037.
[13] H.M. Kim, B.R. Cho, Chem. Commun. 2 (2009) 153–164.
[14] F. Terenziani, C.L. Droumaguet, C. Katan, O. Mongin, M.B. Desce, Chem. Phys. Chem. 8 (2007) 723–734.
[15] H. Detert, M. Lehmann, H. Meier, Materials 3 (2010) 3218–3330.
[16] M. Drobizhev, A. Karotki, Y. Dzenis, et al., J. Phys. Chem. B 107 (2003) 7540–7543.
[17] V. Anand, B. Sadhasivam, R. Dhamodharan, New J. Chem. 42 (2018) 18979–18990.
[18] E. Piovesan, L.B. Boni, E. Ishow, C.R. Mendonca, Chem. Phys. Lett. 498 (2010) 277–280.
[19] R. Lartia, C. Allain, G. Bordeau, et al., J. Org. Chem. 73 (2008) 1732–1744.
[20] X. Gan, Y. Wang, X. Ge, et al., Dye. Pigment. 120 (2015) 65–73.
[21] T. Ishii, T. Isozaki, S. Kinoshita, et al., J. Phys. Chem. A 125 (2021) 1688–1695.
[22] Y. Gong, G.L. Hou, X. Bi, et al., J. Phys. Chem. A 125 (2021) 1870–1879.
[23] H. Chen, L. Wang, W. Wang, et al., RSC Adv. 6 (2016) 97063–97069.
[24] W. Deng, H. Qu, Z. Huang, et al., Chem. Commun. 55 (2019) 2210–2213.
[25] S.R. Marder, L.T. Cheng, B.G. Tiemann, et al., Science 263 (1994) 511–514.
[26] T. Kim, K Lee, Macromol. Rapid Commun. 36 (2015) 943–958.
[27] A. Mishra, M.K.R. Fischer, P. Bauerle, Angew. Chem. Int. Ed. 48 (2009) 2474–2499.
[28] Y. Zhang, J. Guo, X. Li, et al., Spectrochim Acta Part A 230 (2020) 118015.
[29] X. Zhang, X. Gan, S. Yao, et al., RSC Adv. 6 (2016) 60022–60028.
[30] C.L. Devi, K. Yesudas, N.S. Makarov, et al., Dye. Pigment. 113 (2015) 682–691.
[31] F. Ricci, F. Elisei, P. Foggi, et al., J. Phys. Chem. C 120 (2016) 23726–23739.
[32] B. Dereka, M. Koch, E. Vauthey, Acc. Chem. Res. 50 (2017) 426–434.
[33] B. An, J. Gierschner, S. Park, Acc. Chem. Res. 45 (2012) 544–554.
[34] M. Klikar, D. Georgiou, I. Polyzos, et al., Dye. Pigment. 201 (2022) 110230.
[35] J. Wei, Y. Li, P. Song, F. Ma, J. Phys. Chem. A 125 (2021) 777–794.
[36] A. Shabashini, V. Ramar, B. Karthikeyan, M.K. Panda, G.C. Nandi, ChemistrySelect 6 (2021) 12300–12308.
[37] M.M. Raikwar, E. Mathew, M. Varghese, I.H. Joe, S.N. Nethi, Photochem. Photobiol. 95 (2019) 931–945.
[38] R.D. Mohbiya, R.R. Mallah, M.C. Sreenath, et al., Opt. Mater. 89 (2019) 178–190.
[39] J. Song, K. Zhao, H. Zhang, C.K. Wang, Mol. Phys. 117 (2018) 672–680.
[40] V.A. Galievsky, S.I. Druzhinin, A. Demeter, et al., ChemPhysChem 6 (2005) 2307–2323.
[41] J. Lei, C. Guo, F. Liu, et al., Dye. Pigment. 170 (2019) 107607.
[42] E. Ripaud, C. Mallet, M. Allain, et al., Tetrahedron Lett. 52 (2011) 6573–6577.
[43] H. Umezawa, S. Okada, H. Oikawa, H. Matsuda, H. Nakanishi, Bull. Chem. Soc. Jpn. 80 (2007) 1413–1417.
[44] M.J. Frisch, G.W. Trucks, H.B. Schlegel HB, et al., Gaussian 16, Revision A.03, Gaussian, Inc, Wallingford CT, 2016.
[45] Y. Yuan, W. Zhou, M. Tian, et al., Dye. Pigment. 188 (2021) 109235.
[46] Q. Li, W. Perrie, Z. Li, S.P. Edwardson, G. Dearden, Opto-Electron. Adv. 5 (2022) 210036.
[47] K. Wang, H. Long, M. Fu, G. Yang, P.X. Lu, Opt. Lett. 35 (2010) 1560–1562.
[48] V. Ramar, K. Balasubramanian, Appl. Phys. A 124 (2018) 779.
[49] G.Y. Zhou, X.M. Wang, D. Wang, et al., Opt. Commun. 190 (2001) 345–349.